ELSEVIER

Journal of Chromatography A, 972 (2002) 3–19

JOURNAL OF CHROMATOGRAPHY A

www.elsevier.com/locate/chroma

Hydrophobic interaction chromatography of proteins I. Comparison of selectivity

Christine Machold, Karin Deinhofer, Rainer Hahn, Alois Jungbauer*

Institute for Applied Microbiology, University of Agricultural Sciences, Muthgasse 18, A-1190 Vienna, Austria

Abstract

Currently, the selection of a hydrophobic interaction chromatography (HIC) sorbent for protein separation purposes is entirely based on empirical means. An attempt was made to characterize different HIC sorbents from various manufacturers. The selectivity was determined by isocratic pulse experiments of a set of reference proteins and an algorithm was developed to classify the sorbents according to their selectivity and hydrophobicity. The obtained semi-quantitative parameters take into account the dependence of salt on adsorption. The sorbent characteristics evaluated with the model proteins were compared to the separation of a real feedstock. A good agreement was achieved between the developed evaluation procedure and the separation behaviour of the real feed stock.

Keywords: Hydrophobic interaction chromatography; Selectivity; Stationary phases, LC; Proteins

1. Introduction

Shepard and Tiselius [1] first reported on hydrophobic interaction chromatography (HIC), observing the retention of dyes in a so-called salting out chromatography, where sulfate and phosphate solutions where present. As a follow up study, Shaltiel and Er-el [2,3] used the term hydrophobic chromatography or hydrophobic affinity chromatography. Hofstee [4] described the method as hydrophobic adsorption chromatography, and finally Hjertén [5] called the method hydrophobic interaction chromatography. Protein separation by HIC was developed in the 1960s and 1970s. Since then, many attempts have been made to study the parameters influencing protein adsorption in hydrophobic interaction chromatography [6–16]. Normalized retention volume of isocratic elution experiments versus salt concentrations are often applied to characterize a chromatographic system. Such simple chromatographic experiments provide a lot of useful information. Melander and Horváth [6] plotted $\ln k'$ versus salt molarity to shed light on protein retention in HIC. As there is a similarity between salting out of proteins and hydrophobic interaction [17,18], the solvophobic theory, firstly described by Green [19], can be applied for interpretation of the curve shape. The hydrophobic contact area between solute and sorbent, the amount of charged residues of the protein, molal surface tension increment of the salt and repulsive forces of the ligand at zero salt molarity contribute to the slope and the intercept of the straight line portion of the plot. The shape of the curve was flat at low ionic strength, but it increased to a steep and straight line at higher ionic strength.

*Corresponding author. Fax: +43-1-3697-615.
E-mail address: jungbaue@hp01.boku.ac.at (A. Jungbauer).

0021-9673/02/$ – see front matter
PII: S0021-9673(02)01077-4

Later, they investigated retention behaviour in gradient elution and confirmed the postulated correlation between increase in salt concentration and/or molal surface tension increment of the salt, respectively, and retention volume [7]. A deviation from this correlation was observed and explained by special binding effects, which the solvophobic theory cannot account for. A plot of the log of the normalized retention volume versus salt concentration resulted in curves reaching a limiting asymptote for high salt concentrations. For an evaluation of these plots, the slope and the intercept of the investigated proteins eluted with different types of salt were listed.

In order to study the influence of protein charge on retention, different types of lysozyme, with only few substituted amino acid residues, have been chromatographed on an HIC column [14]. Again, the normalized retention volume was plotted versus the salt concentration. The resulting lines were parallel, but the intercept was different for each lysozyme type. Thus the hydrophobic contact area remained the same but the strength of interaction was dependent on the charge varying with amino acid substitution. The same results were obtained by changing the pH of the mobile phase. Changes in the ionization state of the protein affected retention. According to these investigations, the interaction between salt ions and protein could not be neglected. The curve shape was in all cases a straight line but data points at low ionic strength were not available. A quantitative evaluation of the curve shift due to changes in protein charge was not done.

Staby and Mollerup [11] investigated retention of lysozyme on hydrophobic interaction media with large through-pores for a broad range of salt concentration in the eluent buffer. They developed a model where $\ln k'$ is dependent on the activity of he protein in the mobile and in the stationary phase. The activity in the mobile phase can be expressed by a modified Debye–Hückel equation and is dependent on the pH and the ionic strength. Plots of $\ln k'$ versus ionic strength were fitted to the postulated model and with the obtained parameters, activities of the solute on various stationary phases can be calculated and compared. U-shaped curves for lysozyme were obtained by plotting $\ln k'$ versus salt concentration instead of straight lines as initially shown by Melander.

A resourceful thermodynamic model to fit retention data is the preferential interaction analysis [12–14]. It accounts additionally for protein–salt interactions, a factor neglected by the solvophobic theory. The model allows the effect of solutes on the observed equilibrium constant to be interpreted in terms of a stoichiometric displacement model. The parameters have direct physical meaning and the number of water molecules and ions released from a hydrophobic surface upon protein adsorption can be calculated. From these data, the reduction of wetted surface area can be estimated, which is a measure for the hydrophobic contact area between the sorbent and the protein. Curve shapes of the plots $\ln k'$ versus salt concentration are straight lines; retention at zero ionic strength was not investigated. All the models used for interpretation of the retention curves are powerful tools to interpret sorbent and solvent properties under various respects. The great number of parameters to consider reflect the complexity of hydrophobic interaction. However, only the influence of salt has been modeled, although it has been made evident that the ligand length and density is extremely important [20–22].

We investigated protein retention on a great number of sorbents of different hydrophobicity and different base matrices over a wide range of ionic strength. Several data points were also collected at very low ionic strength to characterize the influence of electrostatic interaction. An appropriate model to fit this data did not exist. Therefore, data were fitted with simple polynomial functions. The area below the curve was used as evaluation criterion, expressing an apparent value for hydrophobicity and selectivity for a given separation system. A comparison of the various HIC sorbents was made using these criteria. This information was then compared to a real system separating acid whey. This approach allowed the comparison of performance of HIC sorbents for the given separation system.

2. Materials and methods

2.1. Materials

2.1.1. Buffers and proteins

All buffer ingredients were from Merck (Vienna, Austria). The model proteins α-lactalbumin, β-lacto-

globulin, bovine IgG, bovine serum albumin, ovalbumin, lysozyme and lactoferrin were purchased from Sigma–Aldrich (Vienna, Austria).

2.1.2. Instrumentation

All experiments were performed on an Äkta-Explorer 100 system (Amersham–Pharmacia Biotech, Uppsala, Sweden) consisting of a compact separation unit and a personal computer running a control system (UNICORN, version 3.1).

2.1.3. Stationary phases

Phenyl Sepharose high-performance (HP), Phenyl Sepharose 6FF high substitution, Phenyl Sepharose 6FF low substitution, Octyl Sepharose 4FF, Butyl Sepharose 4FF, Hexyl-*S*-Sepharose 6FF, Butyl-*S*-Sepharose 6FF, Pyridyl-*S*-Sepharose 6FF, Methyl Sepharose 4FF and Butyl Sepharose HP were a gift from Amersham–Pharmacia. Toyopearl butyl 35 μm, Toyopearl butyl 65 μm and Toyopearl phenyl 35 μm were purchased from TosoHaas (Stuttgart, Germany), Macro-Prep Methyl and Macro-Prep *t*-Butyl were purchased from Bio-Rad (Hercules, CA, USA).

2.2. Methods

2.2.1. Isocratic runs

Two ml of each sorbents were filled into HR5/10 columns (AP Biotech) and packed at a flow velocity of 450 cm/h. The bed volume varied between 1.8 and 2 ml.

A 20 m*M* Na-PO_4 buffer, pH 7.0 was prepared as elution buffer. The salt buffer was $(NH_4)_2SO_4$ at various concentrations dissolved in 20 m*M* Na-PO_4 buffer, pH 7.0. The buffers were filtered and degassed prior to chromatography. Isocratic runs were designed as follows: after equilibration of the columns (3 column volumes, CV) at a flow velocity of 306 cm/h with $(NH_4)_2SO_4$ buffer of desired molarity, a 50-μl pulse of the protein sample was injected. The elution volume was 6 CV at a linear flow velocity of 100 cm/h. Regeneration was effected with 20 m*M* Na-PO_4 buffer, pH 7.0. The desired salt concentration the eluent buffer was obtained by mixing 1.0 *M* $(NH_4)_2SO_4$ with 20 m*M* Na-PO_4 pH 7.0. The proteins were dissolved in the respective buffer with ammonium sulfate. Final protein concentration was 5 mg/ml for ovalbumin, 3 mg/ml for α-lactalbumin and bovine serum albumin (BSA) and 2 mg/ml for IgG, lactoglobulin, lactoferrin and lysozyme.

2.2.2. Separation of acid whey

Acid whey was prepared from non-homogenized milk. The milk was centrifuged in a bucket centrifuge Beckman Coulter Avanti J-25 (Beckman Instruments, Palo Alto, CA, USA) at 4420 *g* at room temperature for 30 min for removing of lipids. The supernatant was filtered through a folded filter No. 595 1/2 from Schleicher and Schüll (Düren, Germany). The whey was produced by titration of the skim milk with 6.5% (v/v) HCl to pH 4.6. The precipitated casein was removed by centrifugation in a bucket centrifuge at 4420×*g* at room temperature for 30 min. Residual fines were removed by filtration through the folded filter. The pH was adjusted to 7.0 with 0.5 *M* NaOH. Prior to chromatography, ammonium sulfate was added to 1 ml of acid whey to reach a final salt concentration of 1.5 *M*. The sample was filtered through a microfilter Minisart N (Sartorius, Göttingen, Germany) with 0.2 μm nominal pore diameter to remove the precipitate formed during addition of ammonium sulfate. HR 5/10 columns were packed with Phenyl Sepharose HP, Phenyl Sepharose 6FF high substitution, Phenyl Sepharose 6FF low substitution, Octyl Sepharose 4FF, Butyl Sepharose 4FF, Toyopearl butyl 35 μm, Toyopearl butyl 65 μm, Toyopearl phenyl 35 μm and Macro-Prep Methyl and connected to an Äkta Explorer 100 system.

Equilibration of the columns was effected with 2 CV of a 20 m*M* Na-PO_4 buffer, pH 7.0, with 1.5 *M* ammonium sulfate buffer added, at a linear flow velocity of 306 cm/h. One ml of the sample was injected at a linear flow velocity of 100 cm/h. Unbound protein was washed out with 2 CV of equilibration buffer. The proteins were eluted by a linear decreasing salt gradient from 1.5 to 0 *M* ammonium sulfate in 20 m*M* Na-PO_4 buffer over 10 CV followed by a regeneration step with 1 ml of 30% isopropanol. The gradient was prepared from a 20 m*M* Na-PO_4 buffer, pH 7.0, with 1.5 *M* ammonium sulfate and a 20 m*M* Na-PO_4 buffer, pH 7.0, added. Fractions were manually collected and analyzed by sodium dodecylsulfate–polyacrylamide gel electrophoresis (SDS–PAGE). Aliquots of the

sample and of each fraction were diluted 1:1 in reducing electrophoresis sample buffer (0.125 *M* Tris–HCl, pH 6.8; 10% (v/v) glycerol; 4% SDS; 0.005% bromphenol blue) and incubated at 4°C for 12 h for complete reduction. Twenty μl of the starting material and the fractions were applied to a 4–20% precast gradient gel (Novex, Invitrogen, Carlsbad, USA). Two μl of a prestained molecular mass marker broad range (Bio-Rad) was loaded on each gel. Electrophoresis was carried out at 125 mV for 2 h. The separated proteins were visualized by Coomassie Blue staining.

3. Theory

Peak data collected from UNICORN system were transformed to ASCII files and further processed. The peaks were fitted with an exponentially modified Gaussian function.

The peak fit form of the function was:

$$y = \frac{a_0}{2a_3} \cdot \exp\left(\frac{a_2^2}{2a_3^2} + \frac{a_1 - x}{a_3}\right) \cdot \left[erf\left(\frac{x - a_1}{\sqrt{2}a_2} - \frac{a_2}{a_3}\right) + \frac{a_3}{|a_3|} \right] \quad (1)$$

where a_0 = area of the peak, a_1 = peak center, a_2 = peak width (>0), a_3 = distortion ($\neq 0$)

The first peak moment was calculated from the estimated parameters. The normalized retention k' has been defined as:

$$k' = \frac{V_r - V_0}{V_0} \quad (2)$$

where V_r is the elution volume given as the first peak moment. V_0 is the void volume. The void volume for each sorbent was determined by injecting small pulses of blue dextran under non-binding conditions. A value of 0.4 was determined for all sorbents. Data points $\ln k'$ versus ionic strength were fitted with polynomial functions of second or third order:

$$\ln k' = a + bI + cI^2 \quad (3)$$

$$\ln k' = a + bI + cI^2 + dI^3 \quad (4)$$

Eqs. (3) and (4) were set up with the estimated parameters and were integrated between ionic strength values 0 and 3. The abscissa was arbitrarily set at zero of $\ln k'$. An illustration of the mathematical procedure is shown in Fig. 1.

For case one, when all $\ln k'$ values >0, Eqs. (5) or (6) were used to calculate the area below the curve:

$$A = \int_0^3 (a + bI + cI^2)\mathrm{d}x \quad (5)$$

$$A = \int_0^3 (a + bI + cI^2 + dI^3)\mathrm{d}x \quad (6)$$

where *a*, *b*, *c* and *d* are the parameters from the fit using the second- or third-order polynomial function.

Case two applies when the curve intercepts the abscissa. Then integration yields a positive and negative area. When the curve was fitted with a second-order polynomial function, the intercept of the fitted curve with the abscissa was calculated using Eq. (7).

$$x_{0,2} = \frac{-b + \sqrt{b^2 - 4ac}}{2c} \quad (7)$$

The area below the curve was then the integral from 0 to the intercept with the abscissa, resulting in a negative value for the area, using Eq. (8):

$$A = \int_0^{\frac{-b+\sqrt{b^2-4ac}}{2c}} (a + bx + cx^2)\mathrm{d}x \quad (8)$$

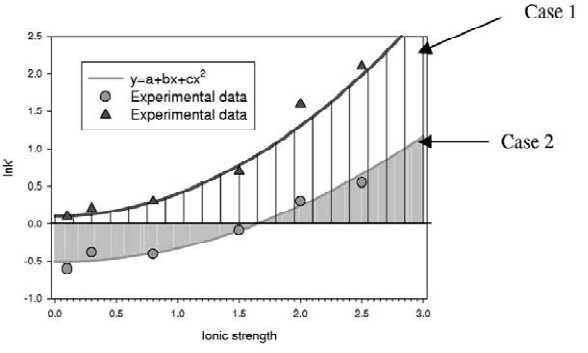

Fig. 1. Illustration of determination of the area below the curve $\ln k'$ versus ionic strength.

and the integral from the intercept with the abscissa to 3, using Eq. (9):

$$A = \int_{\frac{-b+\sqrt{b^2-4ac}}{2c}}^{3} (a + bx + cx^2)\mathrm{d}x \quad (9)$$

Often, the data could be better fitted by using a third-order polynomial function. The intercept with the abscissa was estimated with the computer program Tablecurve 2.4. Positive and negative areas were calculated by using Eqs. (10) and (11):

$$A = \int_{0}^{\text{intercept}} (a + bx + cx^2 + dx^3)\mathrm{d}x \quad (10)$$

$$A = \int_{\text{intercept}}^{3} (a + bx + cx^2 + dx^3)\mathrm{d}x \quad (11)$$

The total area and the ratio of the negative to positive area were used as further evaluation criterion of the HIC sorbents. Scatter of the total areas for all proteins for each sorbent was used as a measure for selectivity. Scatter was expressed as sum of squares, calculated using Eq. (12):

$$s^2 = \frac{\sum (x_i - m_x)^2}{F} \quad (12)$$

where s^2 is sum of squares; x_i is area below the curve for one protein m_i is mean for area below the curve of all proteins; F is degree of freedom, $F = n - 1$; n is number of areas.

The positive area was used to estimate the relative hydrophobicity. The stronger the interaction between sorbent and protein, the higher is $\ln k'$, resulting in large positive areas. To evaluate the hydrophobicity, the mean of all areas for one sorbent was calculated according to Eq. (13):

$$m_x = \frac{\sum x_i}{n} \quad (13)$$

where m_x is mean; $x_i$is positive area below the curve for a particular protein; n is degree of freedom.

4. Results and discussion

4.1. Rational of selection of sorbents

A plethora of different HIC media are commercially available, making the choice of the best suited sorbent for a given separation problem a challenging task. Guidelines can hardly be given because of individually interacting factors between sorbent, protein and eluent. A well suited methodology to characterize different media with modest experimental work is presented here. The matrix of the selected sorbents is based either on agarose, methacrylate or polystyrene. Ligands consist of short alkyl or aryl chains with varying hydrophobic interaction. Ether-, methyl-ligands are known to have a weak interaction with proteins, butyl-, phenyl- and octyl-ligands have a strong one [4]. The density of the ligands and particle size are variable as well. Therefore, a reasonable selection of available HIC sorbents was done to compare differences in base matrix, type and density of ligand and particle size (Table 1). Although selectivity should not be affected by the particle size, preliminary experiments showed contrary results. The ligand density and immobilization chemistry may slightly vary with particle size. All Sepharose sorbents are based on agarose, whereas the Toyoperal and Bio-Rad sorbents are metacrylate sorbents. A broad range of different ligands was tested: phenyl-, octyl-, butyl-, pyridyl-, hexyl-, and methyl-chains. Influence of ligand density was compared by testing Phenyl Sepharose 6FF high sub and Phenyl Sepharose 6FF low sub. To assess the selectivity, seven reference proteins (α-lactalbumin, β-lactoglobulin, bovine IgG, BSA, ovalbumin, lysozyme and lactoferrin) with different properties regarding size, hydrophobicity, and isoelectric point were selected (Table 2).

4.2. Pulse response experiments

Small pulses were injected and chromatographed at different concentrations of ammonium sulfate. The retention volume was determined as the first peak moment and the normalized retention $\ln k'$ was calculated according to Eq. (1). $\ln k'$ values for each protein were plotted against ionic strength. In Fig. 2A–C the plots for all selected sorbents are shown.

Table 1
Properties of the selected sorbents

Sorbent	Base matrix	Ligand type	Ligand density (μmol/ml gel)	Particle size (μm) mean; range
Phenyl Sepharose HP	Cross linked agarose 6%	Phenyl	25	34;24–44
Phenyl Sepharose 6FF high sub	Cross linked agarose 6%	Phenyl	40	90;45–165
Phenyl Sepharose 6FF low sub	Cross linked agarose 6%	Phenyl	20	90;45–165
Pyridyl-*S*-Sepharose 6FF*	Cross linked agarose 6%	*S*-Pyridyl	n.a	90;45–165
Octyl Sepharose 4FF	Cross linked agarose 4%	Octyl	5	90;455–165
Hexyl-*S*-Sepharose 6FF*	Cross linked agarose 6%	*S*-Hexyl	7.8	90;45–165
Butyl Sepharose 4FF	Cross linked agarose 4%	Butyl	50	90;45–165
Butyl Sepharose HP	Cross linked agarose 6%	*n*-Butyl	n.a	34
Butyl-*S*-Sepharose 6FF	Cross linked agarose 6%	*S*-Butyl	n.a	90;45–165
Methyl-Sepharose 4FF	Cross linked agarose 4%	Methyl	n.a	90;45–165
Toyopearl Butyl 65 μm	Polymethacrylate	Butyl	n.a	65;40–90
Toyopearl Butyl 35 μm	Polymethacrylate	Butyl	n.a	35;20–40
Toyopearl Phenyl 35 μm	Polymethacrylate	Phenyl	n.a	35;20–40
Macro-Prep *t*-Butyl	Polymethacrylate	Butyl	n.a	50
Macro-Prep Methyl	Polymethacrylate	Methyl	n.a	50

*Custom-designed media; n.a., not available; Δ, estimated.

The curve pattern in each plot is very different reflecting the different interaction behaviour between sorbent and protein due to sorbent properties only. All other influencing parameters such as pH, temperature and chromatographic conditions were kept constant. Curves vary in their steepness, flexion, position with regard to the ordinate and in their length. For lysozyme the curve was always U-shaped, whereas for all other proteins, the shape was sigmoid. This retention behaviour may be due to electrostatic interactions playing a predominant role at low ionic strength as previously reported [9,23]. Lysozyme is the only negatively charged protein at pH 7.0 and electrostatic attraction may be a reason for the high $\ln k'$ values at low ionic strength. All other model proteins are positively charged and the curve is bent downwards at low ionic strength. The charge of the protein at working pH cannot be neglected for the evaluation of $\ln k'$ at low salt concentrations. The extent of the flexion can be a considered as a measure of electrostatic interaction of the base matrix with the protein. The position of the curve of the Sepharose sorbents (Phenyl Sepharose HP, Phenyl Sepharose 6FF high substitution, Phenyl Sepharose 6FF low substitution, Octyl Sepharose 4FF, Butyl Sepharose 4FF) was slightly higher than of Hexyl-*S*-Sepharose 6FF, Butyl-*S*-Sepharose 6FF, Pyridyl-*S*-Sepharose 6FF, Methyl Sepharose 4FF and Butyl Sepharose HP. For all Toyoperal sorbents and Macro-Prep sorbents a generally lower position of the curves was observed. A ranking according to $\ln k'$ values over the whole range of ionic strength of the single protein curves is difficult because of the different curve shape. However, a general trend can be observed, although in several cases, a selectivity reversal was observed. This means that the investigated HIC resins do not adsorb solely the proteins according to their hydrophobicity, but also a bio-specific interaction may take place. Huang et al. [22] have shown that adsorption of proteins on butyl ligands is enthalpy driven, while on octyl ligands they were entropy driven. It was hypothesized that the octyl ligand may penetrate the protein during adsorption process. Not all proteins are affected to this penetration process to the same extent. Furthermore, some proteins are more com-

Table 2
Properties of the selected model proteins [28]

Proteins	M_r	p*I*	Hydropathicity (GRAVY)
α-Lactalbumin (bovine)	14 200	4.9	−0.151
β-Lactoglobulin (bovine)	18 280	4.9	−0.01
IgG (bovine)	150 000	6.3–7.3	
BSA	66 400	5.8	−0.458
Ovalbumin ((chicken)	42 700	5.19	−0.06
Lysozyme (chicken)	14 300	9.13	−0.542
Lactoferrin (bovine)	78 000	8.7	−0.289

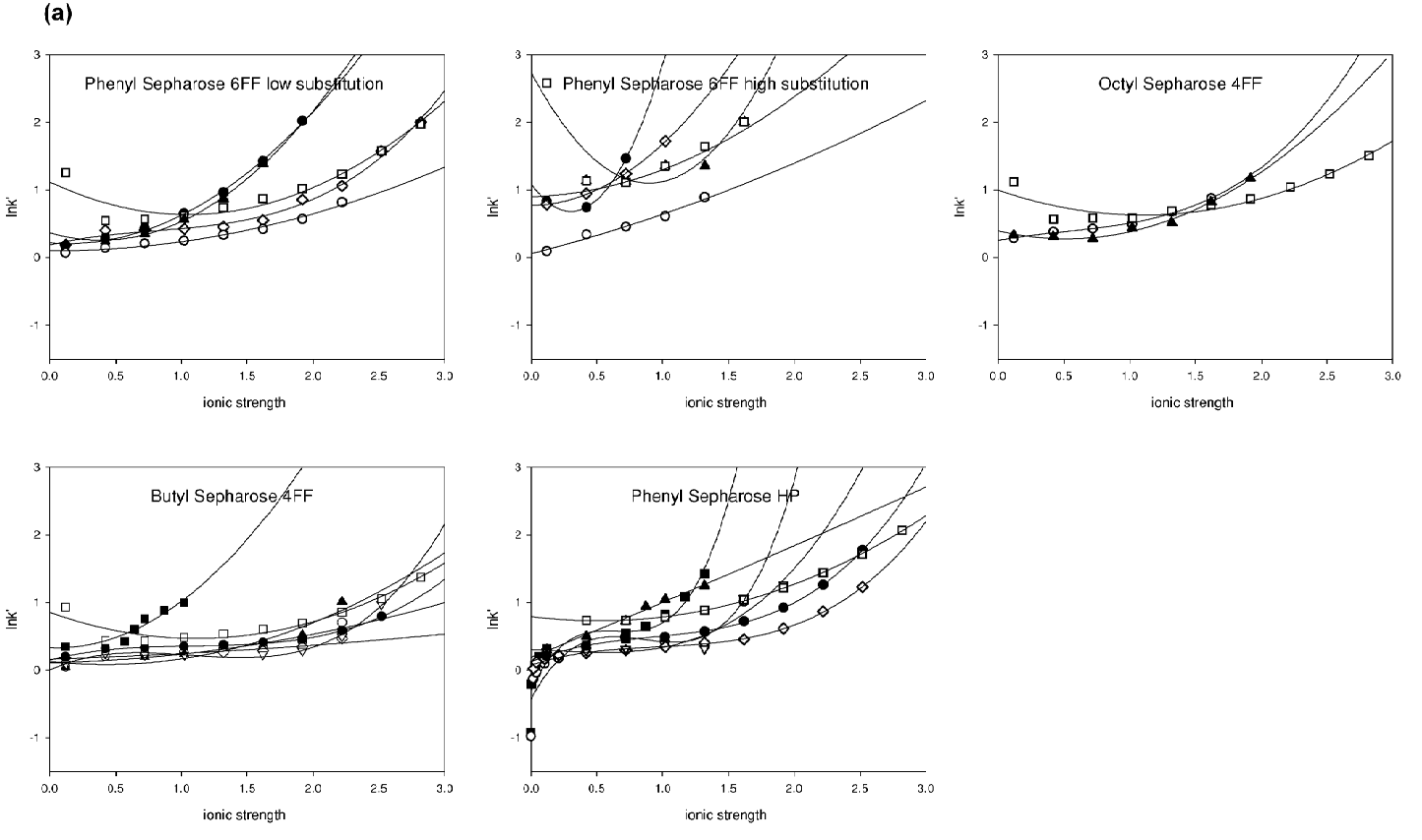

Fig. 2. Plots of ln k' versus ionic strength for (A) five different Sepharose sorbents, (B) five different Sepharose sorbents and (C) three different Toyopearl and two different Macro-Prep sorbents. (■) Lactalbumin, (▲) IgG, (●) BSA, (◇) lactoglobulin, (▽) lactoferrin, (○) ovalbumin, (□) lysozyme.

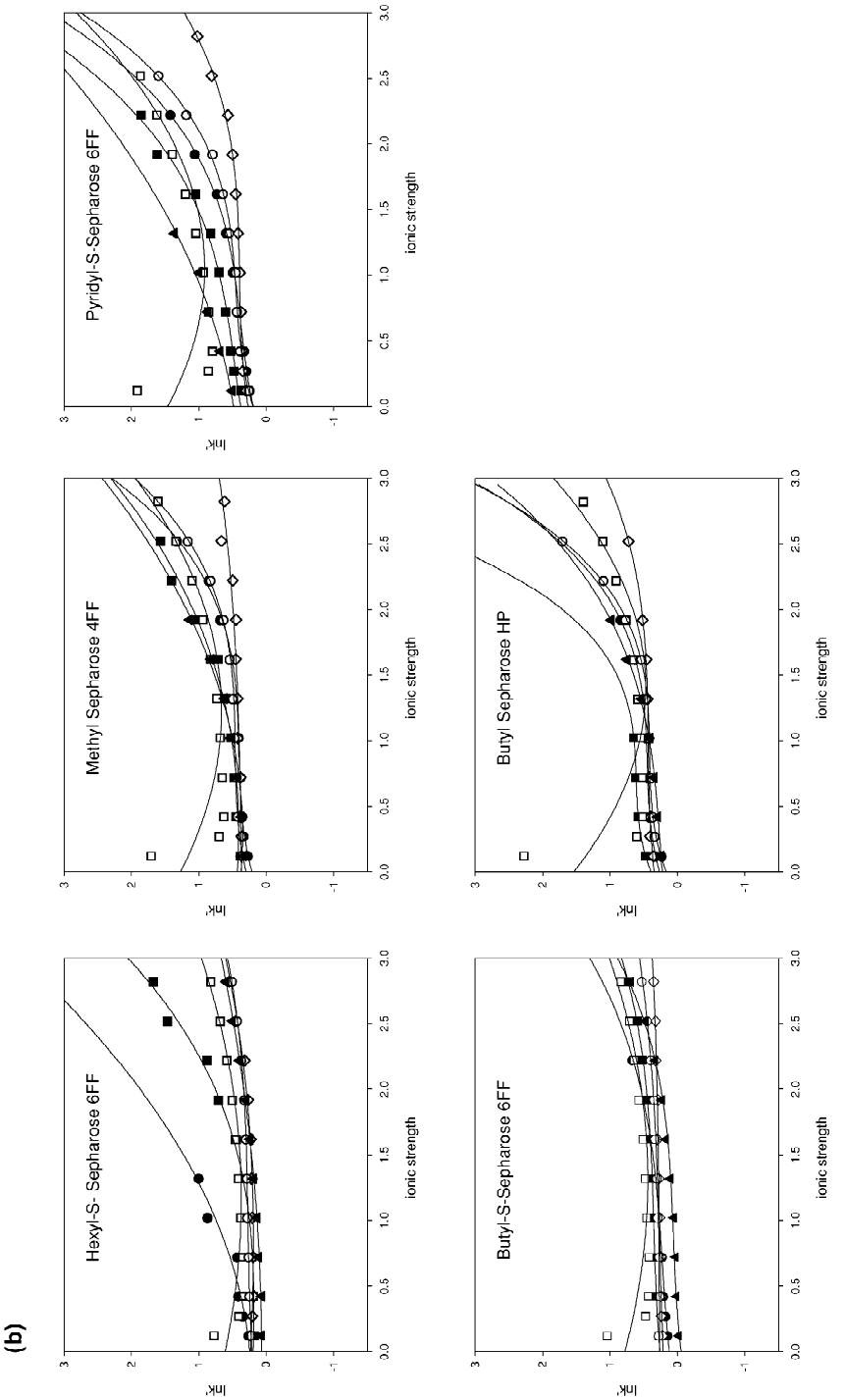

Fig. 2. (*continued*)

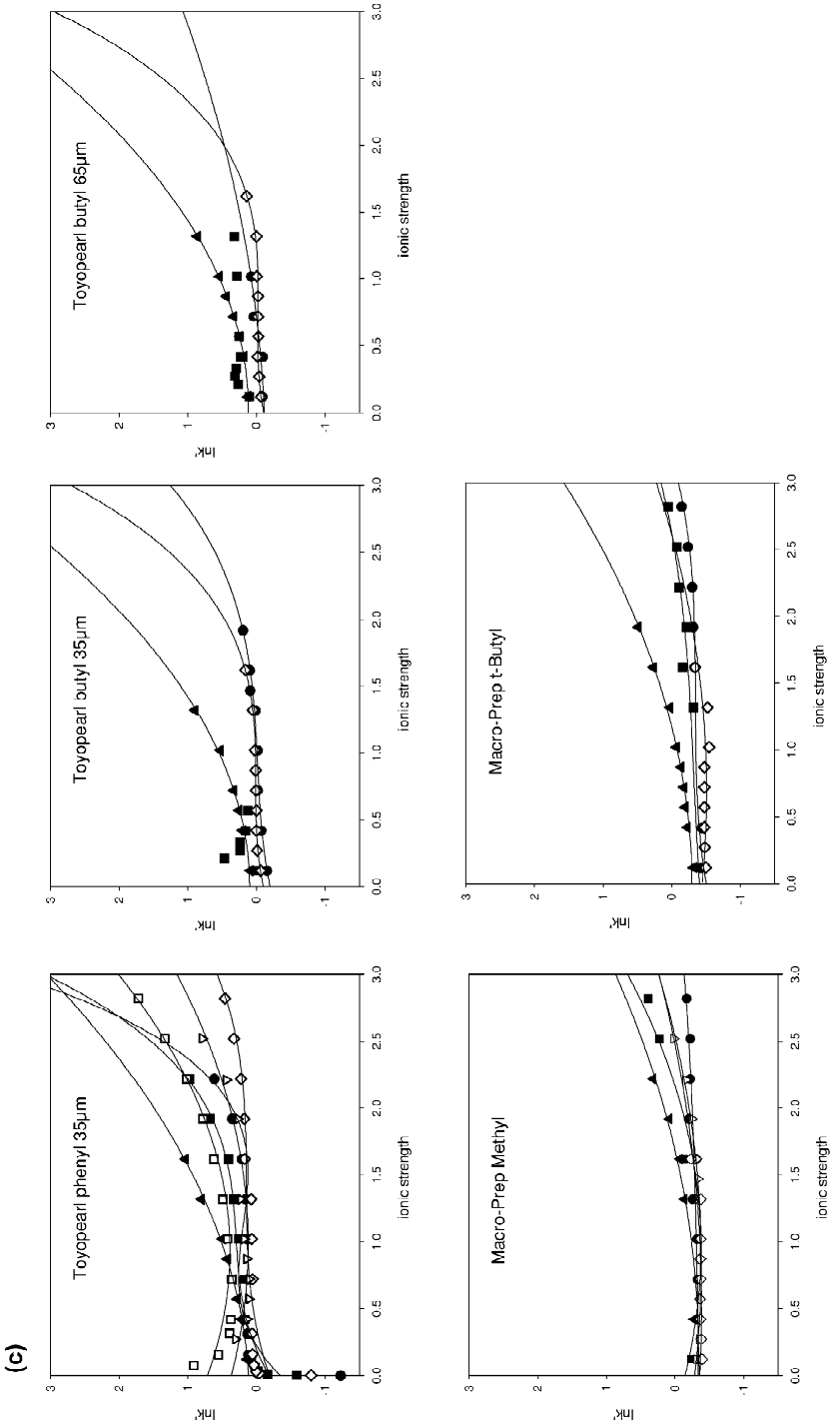

Fig. 2. (*continued*)

pactly folded than others as indicated by their different melting temperature. α-Lactalbumin and IgG were retarded strongest. Interestingly, IgG exerted weak interaction with Hexyl-*S*-Sepharose and Butyl-*S*-Sepharose as shown by $\ln k'$ versus ionic strength curve, while IgG showed modest to strong interaction with all other sorbents. Pyridyl-*S*-Sepharose, a sorbent designed for antibody purification showed high affinity for IgG similar to a lot of other tested sorbents. The curve for lactoglobulin is the one with the lowest $\ln k'$ values for each sorbent with exception of Phenyl Sepharose 6FF high substitution and Phenyl Sepharose 6FF low substitution. Retention behaviour of ovalbumin is comparable to lactoglobulin and the curves are very similar in shape and position. BSA, lysozyme, and lactoferrin are positioned between curves for IgG–lactalbumin and ovalbumin–lactoglobulin. In some experiments lactoferrin showed aberrant behaviour, especially at high ionic strength. A very broad peak with shoulder, particularly split was observed. This is a strong indication that refolding is going on during chromatography [24]. It was decided not to use lactoferrin in most of the experiments, since this protein is not well suited as model protein. Position of the data points $\ln k'$ versus ionic strength can be used as guidance for the extent of hydrophobic interaction sites between the protein and the ligand. It seems that IgG and lactalbumin exhibit stronger interaction than BSA and lysozyme. Ovalbumin and lactoglobulin exhibit weaker interactions.

4.3. Area below the curve

Description and interpretation of the curve shape

Table 3
Arbitrary values for the positive and negative area below the curve for each sorbent and protein

	BSA	α-Lactalbumin	β-Lactoglobulin	Lysozyme	Ovalbumin	IgG	Lactoferrin
Phenyl Sepharose 6FF high sub	n.a	n.a	10.44	10.14	3.18	6.03	n.a
			0.00	0.00	0.00	0.00	
Phenyl Sepharose 6FF low sub	5.01	n.a	2.45	3.17	1.53	5.16	
	0.00		0.00	0.00	0.00	0.00	
Phenyl Sepharose HP	10.01	26.08	1.99	3.46	2.88	4.28	4.10
	−0.03	−0.01	0.00	0.00	0.00	0.00	0.00
Pyridyl-*S*-Sepharose 6FFF	3.07	4.13	1.54	4.18	2.64	5.17	n.d
	0.00	0.00	0.00	0.00	0.00	0.00	
Octyl Sepharose 4FF	n.a	n.a	n.a	2.72	3.62	3.14	n.a
				0.00	0.00	0.00	
Hexyl-*S*-Sepharose 6FF	4.40	1.98	0.87	1.57	0.98	0.80	n.d
	0.00	0.00	0.00	0.00	0.00	0.00	
Butyl Sepharose 4FF	1.28	7.53	5.48	2.25	1.50	1.67	1.45
	0.00	0.00	0.00	0.00	0.00	0.00	0.00
Butyl Sepharose HP	2.82	5.19	1.60	2.64	2.64	2.80	n.d
	0.00	0.00	0.00	0.00	0.00	0.00	
Butyl-*S*-Sepharose 6FF	1.44	1.31	0.86	1.79	1.03	0.66	n.d
	0.00	0.00	0.00	0.00	0.00	−0.01	
Methyl-Sepharose 4FF	2.20	2.83	1.41	3.00	2.13	2.94	n.d
	0.00	0.00	0.00	0.00	0.00	0.00	
Toyopearl Butyl 6 μm	1.02	n.a	1.61	n.d	n.d	4.25	n.d
	−0.05		−0.04			0.00	
Toyopearl Butyl 3 μm	0.73	n.a	1.53	n.d	n.d	4.32	n.d
	−0.08		−0.02			0.00	
Toyopearl Phenyl 3 μm	1.90	2.24	0.52	2.38	n.d	3.45	1.114
	−0.04	−0.02	−0.03	0.00		0.00	0.00
Macro-Prep *t*-Butyl	0.00	0.03	0.04	n.d	n.d	1.23	n.a
	−0.99	−0.66	−0.99			−0.23	
Macro-Prep Methyl	0.00	0.26	0.06	n.a	n.d	0.51	0.05
	−0.82	−0.59	−0.70			−0.40	−0.73

n.d., not determined; n.a., not applicable.

patterns is difficult to interpret in a straight manner. A quantitative value of the interaction between a protein and a sorbent can be obtained from the area below the selectivity curve. These values do not have a direct physical meaning, although the larger the area the stronger the interaction. Expressing curve shape in values for area below the curve allows a ranking of sorbents for a given separation system. The area below each curve has been calculated according to Eqs. (3)–(11). Values for the areas are listed in Table 3. Although a certain reduction of the data for this evaluation is necessary, distribution of values furnish a good overview about selectivity and hydrophobicity. The sum of the absolute values for negative and positive areas is dependent on the steepness of the curve; the steeper the curve, the larger the area. The steepness itself is dependent on the salt influence on protein retention and is an indication of a high selectivity of the sorbent. A sorbent where the areas are different for each protein and the ratio of negative to positive area varies from protein to protein can be classified as highly selective. Curves of $\ln k'$ versus ionic strength are steep and well separated from each other. For further evaluation of the selectivity, the sum of squares of the areas below the curve for each protein was determined for each sorbent according to Eq. (12). This procedure leads to arbitrary numbers and a ranking of the sorbents according to their selectivity towards the investigated model proteins is possible. One has to consider a certain loss of information for this evaluation. In some cases, areas could not be calculated because data did not fit a polynomial function of second or third order. This was the case for lactalbumin on Toyopearl butyl 35 μm and Toyopearl butyl 65 μm so data for the area below the curve were not available.

Data of sum of squares for the area below the curve are shown in Table 4. The sum of squares for Phenyl Sepharose HP was extremely high compared to the other tested sorbents. This was primarily due to the very steep curve for lactalbumin resulting in a larger area below the curve than for the rest of the proteins on this sorbent. Thus, Phenyl Sepharose HP can be regarded as selective for lactalbumin. Phenyl Sepharose high substitution was the only sorbent with a steep curve for lactoglobulin and therefore, this sorbent is ranked on second position concerning selectivity. Three sorbents with butyl ligands (Butyl Sepharose 4FF, Toyopearl butyl 35 μm and Toyopearl butyl 65 μm) are ranked after Phenyl Sepharose high substitution. Particle size seems to have only minor influence on selectivity because the value of the sum of squares for the Toyopearl sorbent with 35 μm particle size is close to the one for the Toyopearl sorbent with 65 μm particle size. However, the values are not identical. Slight variation in ligand density may be a reason for that. Ligand density could play a more important role on selectivity as shown by the comparison between Phenyl Sepharose high substitution, ranked on second position and Phenyl Sepharose low substitution, which is on sixth position. The rather low sum of square value for Octyl Sepharose 4FF may be due to the high hydrophobicity and is not suited for a resolution of the model proteins. The Macro-Prep sorbents exhibited the lowest selectivity among all tested sorbents.

Table 4
List of sorbents ranked according to their sum of squares

Sorbent	Sum of squares (s^2)
Phenyl Sepharose HP	73.71
Phenyl Sepharose 6FF high substitution	16.85
Butyl Sepharose 4FF	6.1
Toyopearl butyl 35 μm	3.43
Toyopearl butyl 65 μm	2.89
Phenyl Sepharose 6FF low substitution	2.53
Hexyl-*S*-Sepharose 6FF	1.87
Pyridyl-*S*-Sepharose 6FF	1.68
Butyl Sepharose HP	1.42
Toyopearl phenyl 35 μm	1.03
Methyl Sepharose 4FF	0.38
Octyl Sepharose 4FF	0.2
Butyl-S-Sepharose 6FF	0.17
Macro-Prep *t*-Butyl	0.1
Macro-Prep Methyl	>0.01

An apparent value for hydrophobicity can be extracted from the ratio of the negative area to the positive area (Table 3). This ratio is affected by the position of the curve. For strongly interacting proteins $\ln k'$ is shifted to a higher position. For quantification of the hydrophobicity, a mean value of the positive area for each protein on one sorbent was calculated according to Eq. (13). When the $\ln k'$ value is negative, the corresponding distribution coefficient is substantially below 1, indicating that interaction is very weak. Thus, considering positive values only does not alter the picture of the hydro-

phobicity range. Lysozyme was excluded from this evaluation because of its electrostatic interaction with the base matrix at low ionic strength resulting in large positive areas. Again, loss of information due to data reduction has to be considered. The values for the mean of all positive areas (m_x) are listed in Table 5. Phenyl Sepharose HP, Phenyl Sepharose 6FF high substitution, Phenyl Sepharose 6FF low substitution and Octyl Sepharose 4FF show highest hydrophobicity. This finding is consistent with the hydrophobicity of the ligand. For phenyl ligands not only hydrophobic but also π–π interactions are described [4], enhancing interaction between protein and sorbent. One exception is Toyopearl phenyl 35 μm, the mean for positive areas is 1.87 and classifies this sorbent as less hydrophobic. Either a low ligand density or a low accessibility of the ligand may explain this behaviour. Pyridyl-*S*-Sepharose can be classified as more hydrophobic as sorbents with butyl ligands. Butyl ligands exhibit milder interactions and it is interesting to find all tested butyl sorbents close together in the rank according to m_x, the parameter of Eqs. (9) and (10). Butyl Sepharose 4FF is followed by Butyl Sepharose HP and Toyopearl butyl 65 μm. Methyl Sepharose 4FF with an m_x similar to the sorbents with butyl ligands, is ranked higher than Toyopearl butyl 35 μm. Only Butyl-*S*-Sepharose 6FF shows different behaviour, it exhibits lower hydrophobicity. The Macro-Prep sorbents are ranked at the end of Table 5. Though Hexyl-*S*-Sepharose 6FF should be a sorbent with rather high hydrophobicity according to the ligand length (C6), m_x is low. This phenomenon may be due to the thiophilic character of the sorbent [15,25,26]. The good agreement with the ranking of the sorbents according to their hydrophobicity expressed in mean values of positive area below the curve and the ranking of ligand hydrophobicity according to their alkyl chain length confirms the applicability of the presented evaluation.

Table 5
List of sorbents ranked according to their means of positive area below the curve

Sorbent	Averaged positive area (m_x)
Phenyl Sepharose HP	8.23
Phenyl Sepharose 6FF high substitution	6.81
Phenyl Sepharose 6FF low substitution	3.54
Octyl Sepharose 4FF	3.38
Pyridyl-*S*-Sepharose 6FF	3.31
Butyl Sepharose 4FF	3.15
Butyl Sepharose HP	3.01
Toyopearl butyl 65 μm	2.33
Methyl Sepharose 4FF	2.30
Toyopearl butyl 35 μm	2.22
Toyopearl phenyl 35 μm	1.87
Hexyl-*S*-Sepharose 6FF	1.8
Butyl-*S*-Sepharose 6FF	1.06
Macro-Prep *t*-Butyl	1.04
Macro-Prep Methyl	0.83

4.4. Real separation system

Acid whey was applied to nine different HIC sorbents. Elution was achieved with a linear gradient of decreasing ammoniumsulfate over 10 CV. Fractions were collected and analyzed by SDS–PAGE. Chromatograms are shown in Fig. 3A,B. Corresponding SDS gels are shown in Fig. 4A,B. The peak profile is very different for each sorbent, only Toyopearl butyl 65 μm and Toyopearl butyl 35 μm show a similar elution pattern. As these sorbents vary in their particle size only, the similarity confirms the reproducibility of the experiments. All proteins of acid whey were adsorbed with exception of Macro-Prep Methyl HIC support. This sorbent has a low dynamic binding capacity and protein break through was due to overloading the column. On all sorbents with phenyl ligands, at least two baseline separated peaks could be determined. Moreover, the first eluting peak is higher than the later eluting peaks. On Phenyl Sepharose 6FF high substitution and Phenyl Sepharose 6FF low substitution the sample elutes in two major peaks, whereas on Phenyl Sepharose HP even four peaks were detected. On the more hydrophobic sorbent, Octyl Sepharose 4FF, just one peak without any shoulders was eluted. For the less hydrophobic sorbents, acid whey proteins eluted in three peaks on Toyopearl phenyl 35 μm, but on Toyopearl butyl 35 μm, Toyopearl butyl 65 μm, Butyl Sepharose 4FF and Macro-Prep methyl support a separately eluting peaks could not be identified. The elution profile of Toyopearl butyl 35 μm and Toyopearl butyl 65 μm was similar and consisted of one peak with only slightly detectable shoulders. On

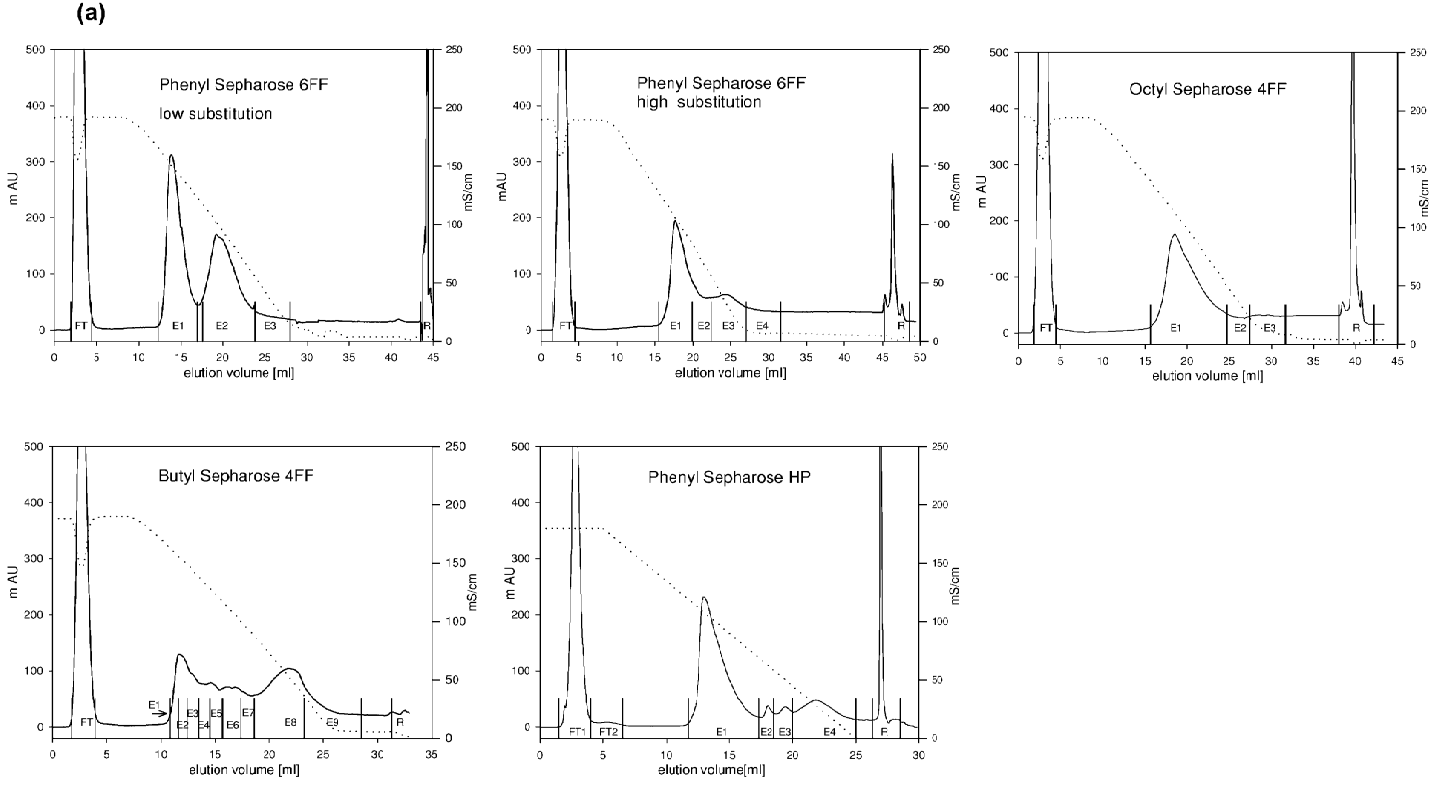

Fig. 3. Chromatograms of acid whey on (A) five different Sepharose sorbents and (B) three different Toyopearl sorbents and one Macro-Prep sorbent. (—) UV line conductivity (mS/cm). FT, flow through; E, eluting fractions; R, regenerate.

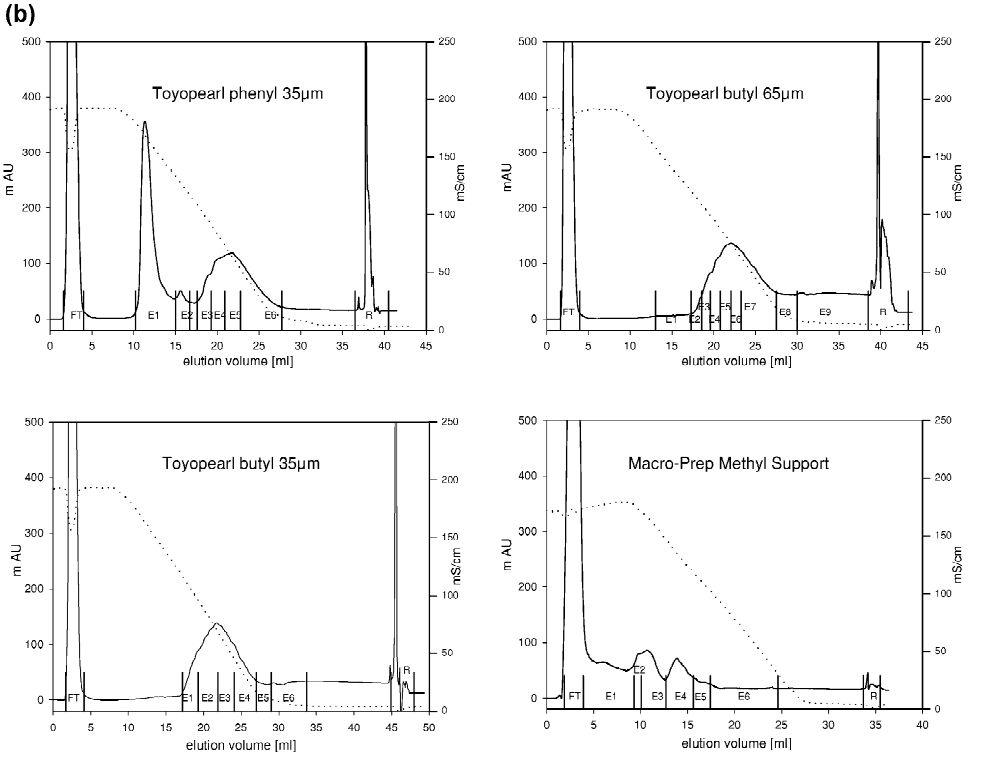

Fig. 3. (*continued*)

Butyl Sepharose 4FF, whey proteins eluted in a broad peak but maxima of peak shoulders could be determined. On Macro Prep Methyl, two very asymmetrical peaks were observed. In cases where more than one peak could be observed, the first peak was always identified as lactoglobulin and peptone by SDS–PAGE. Elution of whey proteins on the different sorbents were compared with the shape and the pattern of the curves $\ln k'$ versus ionic strength of the reference proteins. Lactoglobulin exhibits weakest interaction with all sorbents because it is found in all first eluting fractions. Consistently, $\ln k'$ values for this protein are in most cases the lowest ones. Furthermore, lactoglobulin is detected in every fraction. The curve is in most cases the flattest one, as a consequence of a weak salt dependency of the protein adsorption. Therefore, elution of lactoglobulin was observed along the whole gradient. Only on Phenyl Sepharose 6FF high substitution, was the curve for $\ln k'$ versus ionic strength for lactoglobulin steep and the $\ln k'$ values higher than for the other investigated reference proteins above an ionic strength of 1. Lactoglobulin was found in the first three eluting fractions (E1–E3) on this sorbent but not in the last one (E4). On Phenyl Sepharose 6FF high substitution and Phenyl Sepharose HP, the curves for lactoglobulin rise up at higher ionic strength, indicating enhanced salt promoted retention. For these two sorbents, lactoglobulin was not detected in the last eluting fraction either. Chromatograms and plots of $\ln k'$ versus ionic strength for the two sorbents Phenyl Sepharose 6FF low substitution and Phenyl Sepharose 6FF high substitution were different; ligand density has an important influence on the retention behaviour. In the second peak eluting from Phenyl Sepharose 6FF low substitution, which was collected as fraction E2, all whey proteins were detected. The curves $\ln k'$ versus ionic strength for all proteins were steep and similar in shape. A separation of the whey proteins into several peaks

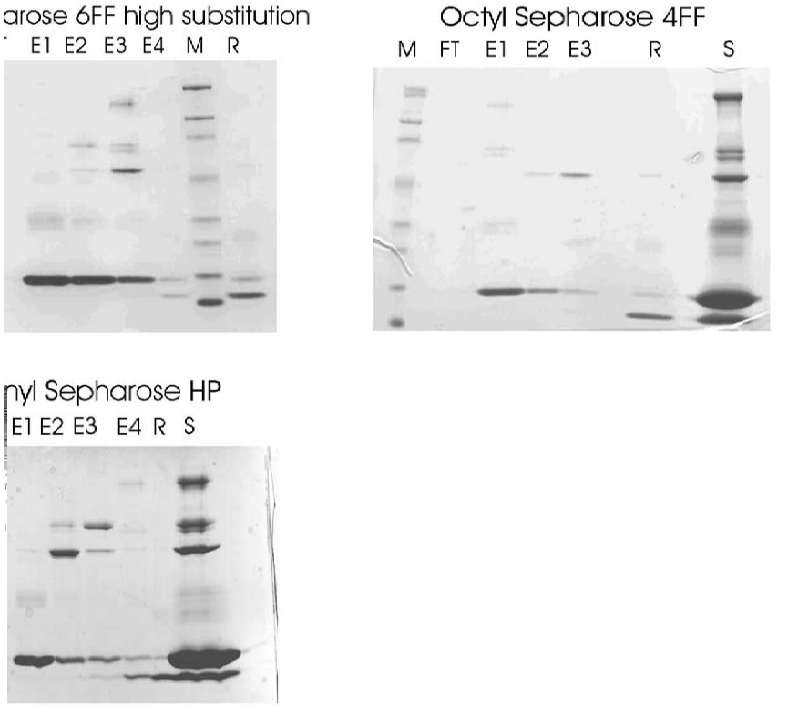

Fig. 4. SDS–PAGE of the collected fractions and original sample from separation of acid whey for (A) five different Sepharose sorbents and (B) three different Toyopearl sorbents and one Macro-prep sorbent. Four to 20% precast gradient gels (Novex); sample volume, 20 μl; dilution, 1:1; S, sample; FT, flow through; E, elution fractions; R, regenerate; M, molecular mass marker proteins.

linear conditions. Extrapolation to non-linear conditions must be made with caution. At non-linear conditions, sample displacement may occur and elution order could be reversed. Further work is necessary to relate these empirical data to characteristics with physical meaning. Hydrophobicity measured as wetting angle is very difficult to assess in porous media. For other feedstocks, the selectivity and interaction strength may change due to biospecific interaction of proteins with the ligand. Another approach to characterise chromatographic media has been proposed by Cramer and co-workers [27]. They applied the concept of molecular descriptors. With this method, they could rank ion-exchange media with regard to strength of interaction. General predictions cannot be made due to the variability of surface proteins of proteins (Tables 4 and 5).

4.5. Conclusion

The described procedure provides a simple interpretation of retention data of proteins on HIC sorbents. The selectivity can be quantified to a limited extent of extrapolation to the separation of real feedstocks.

Acknowledgements

The financial support of Amersham Pharmacia Biotech is gratefully acknowledged.

References

[1] C.C. Shepard, A. Tiselius, in: Discussions of the Faraday Society, Vol. 7, Hazell Watson and Winey, London, 1949, p. 275.
[2] S. Shaltiel, Z. Er-el, Proc. Natl. Acad. Sci. USA 52 (1973) 778.
[3] S. Shaltiel, Z. Er-el, Proc. Natl. Acad. Sci. USA 52 (1973) 430.
[4] B.H.J. Hofstee, Anal. Biochem. 52 (1973) 430.
[5] S. Hjertén, J. Chromatogr. 87 (1973) 325.
[6] W.R. Melander, Cs. Horváth, Arch. Biochem. Biophys. 183 (1977) 200.
[7] W.R. Melander, Cs. Horváth, J. Chromatogr. 317 (1984) 67.
[8] J. Porath, J. Chromatogr. 376 (1986) 331.
[9] B.F. Roettger, M.R. Ladisch, Biotech. Adv. 7 (1989) 15.
[10] W.R. Melander, Z. El Rassi, Cs. Horváth, J. Chromatogr. 469 (1989) 3.
[11] A. Staby, J. Mollerup, J. Chromatogr. A 734 (1) (1996) 205.
[12] T.W. Perkins, D.S. Mak, T.W. Root, E.N. Lightfoot, J. Chromatogr. A 766 (1997) 1.
[13] S.L. Wu, A. Figueroa, B.L. Karger, J. Chromatogr. 371 (1986) 3.
[14] J.L. Fausnaugh, F.E. Regnier, J. Chromatogr. 359 (1986) 131.
[15] P.P. Berna, N. Berna, J. Porath, S. Oscarsson, J. Chromatogr. A 800 (2) (1998) 151.
[16] M.L. Heinitz, L. Kennedy, W. Kopaciewicz, F.E. Regnier, J. Chromatogr. 443 (1988) 173.
[17] M. Dixon, E.C. Webb, Adv. Protein Chem. 16 (1961) 197.
[18] R.K. Scopes, in: C.R. Cantor (Ed.), Protein Purification—Principle and Practice, 3rd ed., Springer, New York, 1994.
[19] A.A. Green, W.L. Hughes, Methods Enzymol. 1 (1955) 67–78.
[20] M.E. Thrash Jr., N.G. Pinto, J. Chromatogr. A 908 (1-2) (2001) 293.
[21] M.A. Esquibel-King, A.C. Dias-Cabral, J.A. Queiroz, N.G. Pinto, J. Chromatogr. A 865 (1-2) (1999) 111.
[22] H.M. Huang, F.Y. Lin, W.Y. Chen, R.C. Ruaan, J. Colloid Interface Sci. 229 (2) (2000) 600.
[23] Z. el Rassi, Cs. Horváth, J. Chromatogr. 326 (1985) 79.
[24] N.S. Mitchell, L. Hagel, E.J. Fernandez, J. Chromatogr. A 779 (1–2) (1997) 73.
[25] S. Oscarsson, J. Porath, J. Chromatogr. 499 (1990) 235.
[26] J. Porath, F. Maisano, M. Belew, FEBS Lett. 185 (2) (1985) 306.
[27] C.B. Mazza, N. Sukumar, C.M. Breneman, S.M. Cramer, Anal. Chem. 73 (22) (2001) 5457.
[28] http://www.expasy.ch/sprot/